PHYSICAL REVIEW B VOLUME 16, NUMBER 8 15 OCTOBER 1977

Hopping transport in a molecularly doped organic polymer

G. Pfister
Xerox Webster Research Center, Webster, New York 14580
(Received 25 March 1977)

Electronic transport in the polycarbonate polymer Lexan molecularly doped with triphenylamine (TPA) has been studied by time-of-flight techniques as a function of temperature, applied field, and TPA concentration. Only hole transport could be observed. The experimental data provide evidence that the transport of holes occurs by a hopping process which connects sites associated with the TPA molecule. The results are analyzed in terms of the theory of stochastic non-Gaussian transport by Scher and Montroll. This theory provides a consistent description of all experimental results if field-induced barrier lowering and temperature-dependent dispersion are formally introduced in the final expression for the transit time.

I. INTRODUCTION

Scher and Montroll[1,2] recently advanced a theoretical framework to describe dispersive transient photocurrents which are observed in an increasing number of both organic and inorganic disordered solids. The present paper discusses time-of-flight experiments on molecularly doped organic polymers which provide a novel class of materials that are ideally suited for detailed experimental examination of the theoretical predictions.[3-7]

The general features of Scher and Montroll's theoretical concept have been verified in detail for hole transport in the amorphous chalcogenides a-As_2Se_3 (Refs. 8 and 9) and a-Se (low temperatures).[10] In particular, the shape of the transient current pulse and the correlated "anomalous" sample thickness and electrical field dependence of the transit time t_T exhibit the predicted functional relationships. Despite the overall agreement with the Scher-Montroll theory, the identification of the microscopic transport mechanism is not straightforward in these materials, since, in its general form, the theory describes the statistics of the process and therefore does not specify the underlying physical mechanism constituting the statistical events. To unravel the details of the transport mechanism, the theoretical concept has to be narrowed to treat specific models. A rather detailed theoretical background exists for hopping transport with a discrete activation energy.[1] Theoretical refinements are in progress to include a distribution of hopping energies and to describe alternative transport mechanisms such as multiple trapping and trap-controlled hopping.[9,11-14] Although these extensions of the theoretical concept will narrow the range of possible interpretations of the transport mechanims, a clear identification would require the experimental modification of materials parameters specific to the proposed transport model, such as the densities of hopping or trapping sites. In this respect, the concept of molecularly doping of organic polymers is extremely powerful.

The first comprehensive study of electron transport in doped polymer systems has been reported for the charge transfer complex of poly(N-vinyl carbazole), PVK, with trinitrofluorenone, TNF.[15] With increasing TNF loading the hole mobility was shown to exponentially decrease from its value for undoped PVK, while in the same concentration range, the electron mobility, which in the undoped PVK is not measurable, exponentially increases. These findings were strong evidence that both carriers in PVK:TNF are transported by a hopping mechanism. While in PVK:TNF the matrix polymer itself is capable of efficient hole transport and, in addition, interacts with the dopant molecule to form a charge transfer complex, such requirements on the host polymer are not necessary. In fact, for some systems, the primary function of the polymer is to provide the (inert) matrix for the solid solution of the dopant molecules. A specific example is the dispersion of N-isopropylcarbazole, NIPC, molecularly dispersed in the polycarbonate polymer Lexan 145 (General Electric trademark).[6] Time-of-flight experiments on NIPC-doped Lexan clearly establish the existence of hole transport which cannot be observed in the undoped polymer. The hole mobility depends exponentially on the NIPC concentration which indicates that carrier transport occurs by a hopping mechanism involving the NIPC molecules as hopping sites. In such systems, therefore, one has the unique opportunity to vary the hopping-site density in a controlled manner. It is furthermore possible to change the molecular entity constituting the

hopping site, study the influence of traps on hopping transport by intentionally doping with an appropriate combination of molecules,[7] and, finally, to examine aspects related to the polymer host matrix such as morphology and polarization.

The present paper expands on the initial studies of hole transport in Lexan doped with donor molecules such as N-isopropylcarbazole,[6] NIPC, or triphenylamine,[7] TPA, and discusses in detail the field, temperature, concentration, and sample thickness dependence of hole transport in TPA-doped Lexan. Section III provides an overview of the experimental findings which are presented in terms of a compact phenomenological expression for the mobility, Eq. (1). The results demonstrate that the activation energy and field dependence of the drift mobility increase with decreasing TPA concentration.

The experimental results are discussed in Sec. IV in terms of current theoretical models. In particular, the Scher-Montroll theory[1,2] of dispersive transport in disordered solids will be examined. It will be shown that a consistent interpretation of the results is obtained when field-induced barrier lowering and temperature-dependent dispersion are formally introduced in the theoretical expression for the transit time.

II. EXPERIMENTAL

A. Samples

Commercially available TPA [$(C_6H_5)_3N$] and polycarbonate polymer (General Electric Lexan 145) were dissolved in weighted amounts in a common solvent, usually 1,2-dichloroethane. After stirring, the mixture was cast in a dry nitrogen ambient onto a ball grained clean aluminum plate (5×7 in.), using a draw-down coating apparatus. The films were dried in vacuum at 315 K for 1–2 h before they were overcoated with semitransparent gold electrodes (0.3 cm^2) to form a sandwich cell. The sample thicknesses were determined from the capacitance measured at 10 kHz and using a dielectric permittivity of $\epsilon = 3$. All films were approximately 10 μm thick.

The TPA concentration referred to in this paper is defined as the weight ratio in grams of TPA to Lexan as it has been introduced into the solution. The concentration range studied was from 0.1 to 0.5 TPA. No signs of crystallization under ambient conditions could be noted in this concentration range. The actual concentration in the sample film was determined from infrared absorption measurements by comparing peak intensities of TPA and Lexan absorptions in the film with a curve calibrated from solution absorption. These studies showed that the concentration of the TPA molecules in the films was lower than in the solution by an amount which increased with increasing TPA (solution) concentration, drying temperature and time, and decreasing film thickness. For example, the loss from a nominal 0.5-TPA film of 7 μm thickness increased from ~2% for one hour drying at 315 K to ~5% at 335 K to ~55% at 370 K. Under similar conditions the loss from a 0.1-TPA film was negligible. As a function of film thickness, the decrease of the actual film concentration became apparent for thicknesses below ~5 μm for 0.5 TPA, 1 h, and 315 K drying conditions. For the preparation conditions used in these experiments (315 K, 1 h, 10 μm) the loss of TPA molecules is insignificant and the solution concentration can be assumed to equal the film concentration. One has to bear in mind, however, that close to the surface (~1 μm) the TPA concentration is expected to be lower than that in the bulk of the film. While this concentration depletion layer may distort the shape of the current pulse as it is observed in the time-of-flight experiment, the effect on the measured transit time is not significant.

Films with the concentrations 0.1, 0.15, 0.2, 0.3, 0.4, and 0.5 TPA were studied, and for each concentration at least two samples were examined. The results were reproducible to a degree which will become apparent from the data shown in Sec. III.

B. Time-of-flight experiments

The details of the experimental procedures used to analyze the dispersive current pulses which are typical for the system under discussion have been described in detail elsewhere.[9,16] In the limit of non-Gaussian statistics, Scher and Montroll predict algebraic time dependences for the transient current $I(t)$ at times $t < t_T$ and $t > t_T$, where t_T is the transit time [see Eq. (3)]. Hence, the salient feature of the analysis of dispersive current transients is a plot of $\log_{10} I$ vs $\log_{10} t$ which allows a direct determination of the power exponents. An operational transit time t_T can then be defined by the intercept of the tangents approximating the current pulse at early and late times.

The carriers were generated by a 5-nsec pulse of 3371 Å wavelength derived from a N_2 laser. At this wavelength Lexan 145 is transparent and the light is exclusively absorbed in the first singlet transition of the TPA molecule. For the concentration range 0.1–0.5 TPA, the absorption coefficient at 3371 Å is $(1-2) \times 10^5$ cm^{-1}, i.e., for all concentrations the light is absorbed within a small fraction of the sample thickness. To minimize distortions of the pulse shape, the light intensity was kept low and

the light flash followed the application of the bias field within a time shorter than ~1 sec.

In a typical experimental run the field dependence of the transit time was first recorded at room temperature. The temperature was then lowered in steps of 5–10 K. Measurements above room temperature were performed only on films with low loading because of the evaporation of the TPA molecules described earlier.

The transit time strongly increases with decreasing TPA concentration and temperature. For this reason it was not possible to investigate all samples in the same temperature range. The samples with low TPA concentration were investigated at higher temperatures than the high-concentration samples. It was, of course, advantageous that the loss of TPA molecules from the film at higher temperatures rapidly decreased with decreasing TPA concentration. Typically, a 0.5-TPA film could be measured in the temperature range 200–300 K, whereas the range for a 0.1-TPA film was 260–360 K. For the same reasoning the range of the applied field varied with concentration, temperature, and sample. At room temperature typical field ranges for the 0.5- and 0.1-TPA films were 15–100 and 40–100 V/μm, respectively.

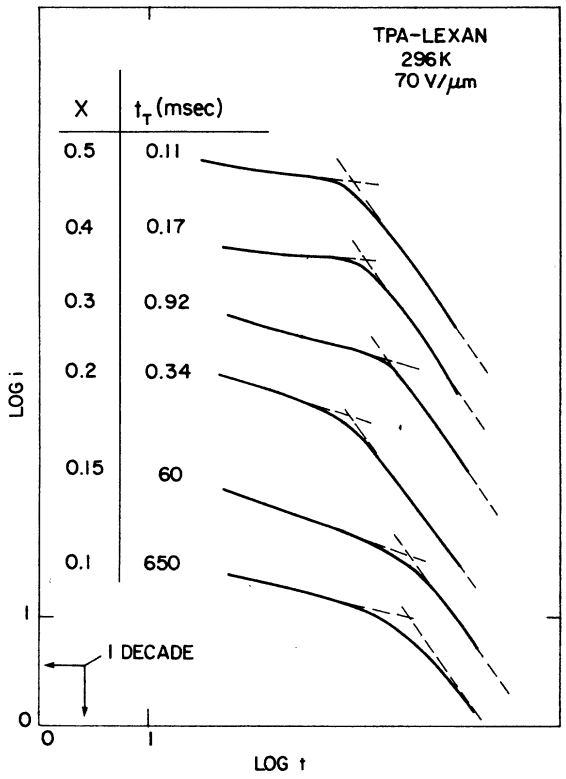

FIG. 1. Transient hole current pulses in units $\log_{10} I$ vs $\log_{10} t$ in TPA-Lexan for various TPA concentrations at $T = 296$ K, and $E = 70$ V/μm. The weight ratios X of TPA to Lexan and the transit time t_T determined from the intercept of the tangents (dashed lines) are listed in the legend.

III. RESULTS

A. Current shape

The shape of the current pulse indicates a broad dispersion of the propagating hole-carrier packet. Following the light flash, the current first drops (initial spike), then levels off (plateau), and finally slowly approaches the dark current level (tail). The behavior of the current in the plateau region exhibited strong variation as a function of the resting history, concentration, and temperature. For some cases (mostly low TPA concentration or low temperatures), the plateau was absent and the shape of the current was essentially featureless. In other cases (mostly high TPA concentrations or high temperatures) a cusp was observed instead of the plateau and the initial spike was significantly sharper but reduced in amplitude. The occurrence of a cusp is usually attributed to field distortions due to space-charge or surface trapping with release times of the order of the transit time.[9,17] Both of these effects are likely to contribute to the pulse distortion in the discussed doped-polymer systems because of the depleted molecule concentration at the gold contact-polymer interface. In the present experiments, samples that gave rise to a large cusp were not further used.

Figure 1 shows transient current traces in logarithmic units recorded at room temperature and 70 V/μm for various TPA concentrations. The main feature of an algebraic time dependence of the current pulse for $t < t_T$, and $t > t_T$, is indicated and the transit time can easily be defined. (In units I vs t the traces for the diluted samples would be quite featureless.) It is noted that the slope describing the tail of the current pulse is relatively insensitive to the TPA concentration. For $t > t_T$ the dashed lines in Fig. 1 were drawn to be parallel. The rounding of $I(t)$ around t_T appears more extended in samples with low TPA concentration. For $t < t_T$ the shape of $I(t)$ varies among the samples in an inconsistent fashion. The transit time t_T, given in the legend of Fig. 1, decreases about 6000 times if the TPA concentration is lowered from 0.5 to 0.1 TPA. As a function of field at constant temperature, the transient current essentially maintains its shape; in particular the tail slopes are quite insensitive to the time frame of the experi-

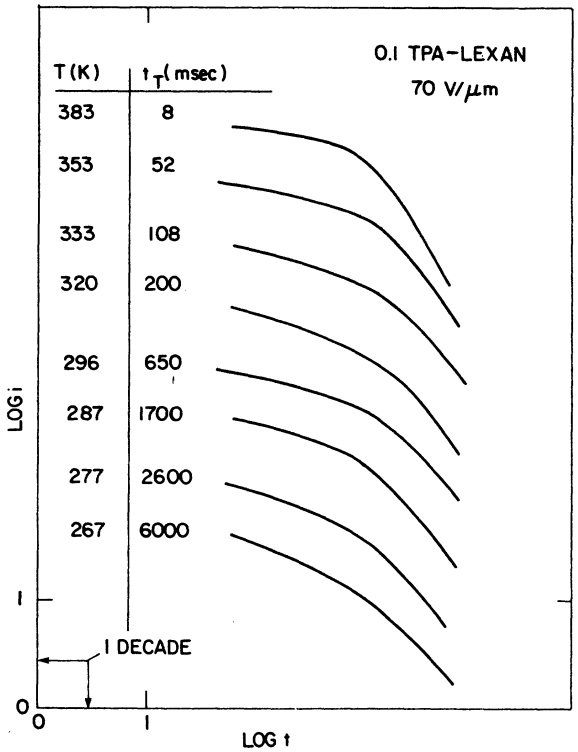

FIG. 2. Transient hole current pulses in units $\log_{10} I$ vs $\log_{10} t$ in 0.1 TPA/Lexan at $E = 70$ V/μm for various temperatures. The temperatures T and the transit time t_T, determined as described in Fig. 1, are listed in the legend.

ment ("universality" of the current shape). Lowering the temperature at constant field generally leads to more dispersive traces and the transition between the two time regimes at $t \sim t_T$ becomes more washed out. Representative current traces as a function of temperature are shown in Fig. 2 for the 0.1 TPA sample.

B. Field and temperature dependence

In the course of organizing the experimental results, it was found that the phenomenological relationship

$$\mu = \mu_0 \exp[(a/k)(E^n - E_0^n)(1/T - 1/T_0)] \qquad (1)$$

provides a useful and convenient description for the field and temperature dependence of the mobility. In Eq. (1), μ_0 depends only upon the TPA concentration, $n \sim \frac{1}{2}$, and a, E_0, and T_0 are parameters. (A similar relationship was found to characterize the electron and hole drift mobility data for the charge transfer complex PVK:TNF.[15]) It is convenient then to represent the data in plots of $\log_{10}\mu$ vs $E^{1/2}$ and $\log_{10}\mu$ vs $1/T$.

The results for a 0.4-TPA sample are chosen to

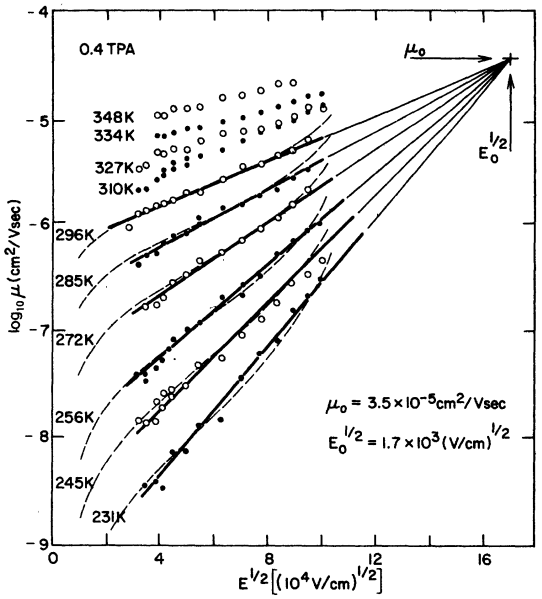

FIG. 3. Field dependence of the hole drift mobility in 0.4 TPA-Lexan for various temperatures. Dashed lines were calculated from Eq. (9) using $\alpha_0 = 0.23$, $\rho = 11.1$ Å, $\Delta_0 = 0.5$ eV, and $T_0 = 435$ K. See Sec. IV B.

illustrate several typical observations. In Fig. 3 the square-root field dependence of $\log_{10}\mu$ is shown for various temperatures. The same results are replotted in Fig. 4 as a function of $1/T$ for various applied fields. In both figures straight lines which have a common intercept at μ_0, $E_0^{1/2}$ and μ_0, $1/T_0$ can be drawn through the appropriate sets of data points, and the values for μ_0 obtained from the two inter-

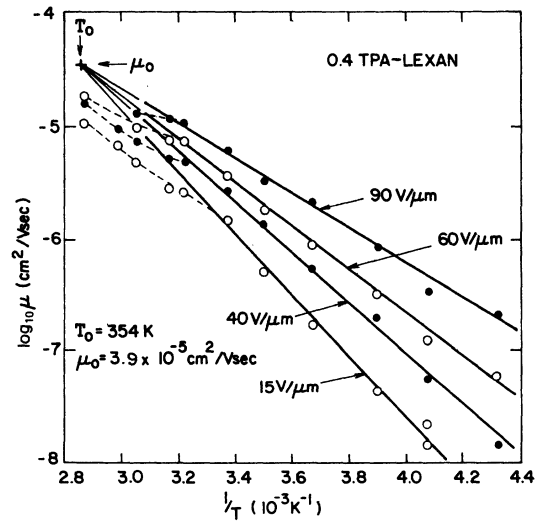

FIG. 4. Temperature dependence of the hole drift mobility in 0.4 TPA-Lexan at various applied fields.

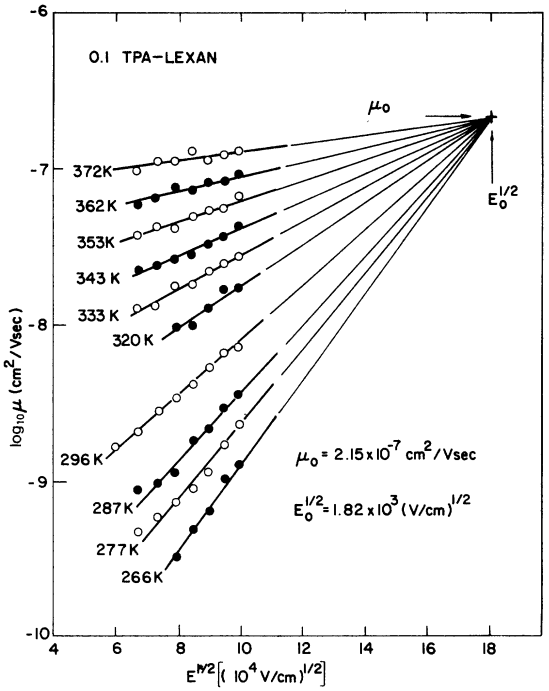

FIG. 5. Field dependence of the hole drift mobility in 0.1 TPA-Lexan for various temperatures.

cepts are in close agreement.

The results for $T \geq 310$ K were not included to determine the common intercept. As is evident from Fig. 4, the temperature dependence of the mobility abruptly weakens above room temperatures. This behavior is believed to be associated with the glass transition which for a 0.4-TPA sample occurs at ~325 K.

Calorimetry measurements on the same TPA-Lexan films show that the glass transition temperature T_g decreases with increasing TPA loading from ~418 K for pure Lexan 145 to ~315 K for the 0.5-TPA sample.[18] For pure TPA, $T_g \sim 250$ K. In agreement with the calorimetry measurements the deviation from the Arrhenius temperature dependence shifted to higher temperatures as the TPA concentration was lowered. Figure 5 shows that for the dilute 0.1 TPA sample, where $T_g \sim 385$ K, Eq. (1) describes the field dependence of the mobility for temperatures ranging up to ~370 K.

In assessing the validity of Eq. (1) one has to consider that the field and temperature range experimentally accessible are quite small. In particular, the exponent n of the field dependence could not be determined rigorously, and for some samples $n = 1$ provided an equally good fit to the data as did $n = \frac{1}{2}$. A more stringent test of Eq. (1) was provided by the plots of the activation energy Δ vs $E^{1/2}$ and of the slope β (Figs. 3 and 5) vs $1/T$. These plots yielded straight lines with intercepts at $E_0^{1/2}$ and $1/T_0$ for $\Delta = 0$, and $\beta = 0$, respectively, which were in good agreement with the values obtained from the intercepts at $\mu_0, E_0^{1/2}$ (Figs. 3 and 5), and $\mu_0, 1/T_0$ (Fig. 4). For a fixed TPA concentration the parameters a, $E_0^{1/2}$, and T_0 as determined for different samples were in agreement to within $\pm 20, \pm 15$, and $\pm 10\%$, respectively.

C. Concentration dependence

In Fig. 6 the mobility values μ_0 obtained from the intercepts at $E_0^{1/2}$ and $1/T_0$ are plotted in units of $\log_{10}(\mu_0/\rho^2)$ versus the average TPA intersite distance which was calculated from the TPA concentration. [In calculating ρ from the TPA concentration, one tacitly assumes a uniform dispersion of pointlike molecules. In actuality, the dimensions of the TPA molecule are of the order of the "hopping" distance and the molecules might be aggregated as dictated by the morphology of the host matrix polymer Lexan 145. Nevertheless, the further analysis will indicate that $\rho \sim (n_{\mathrm{TPA}})^{-1/3}$ is a reasonable measure of the hopping distance.]

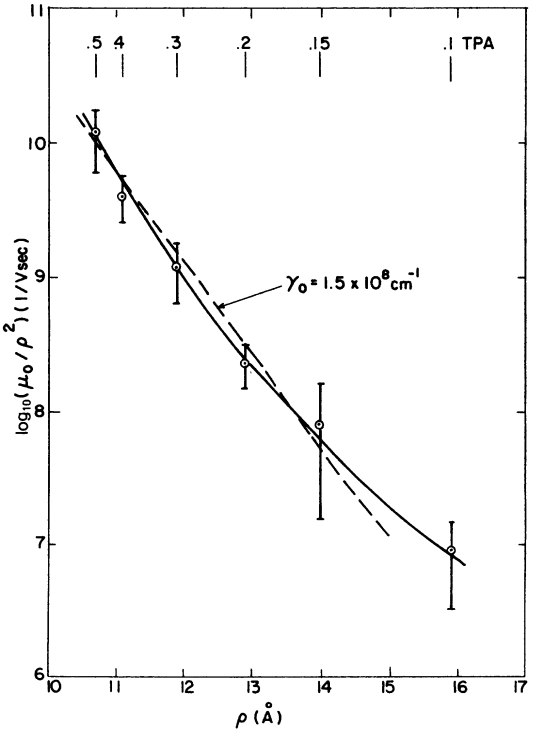

FIG. 6. Concentration dependence of the hole mobility μ_0 determined from the intercepts illustrated in Figs. 3–5.

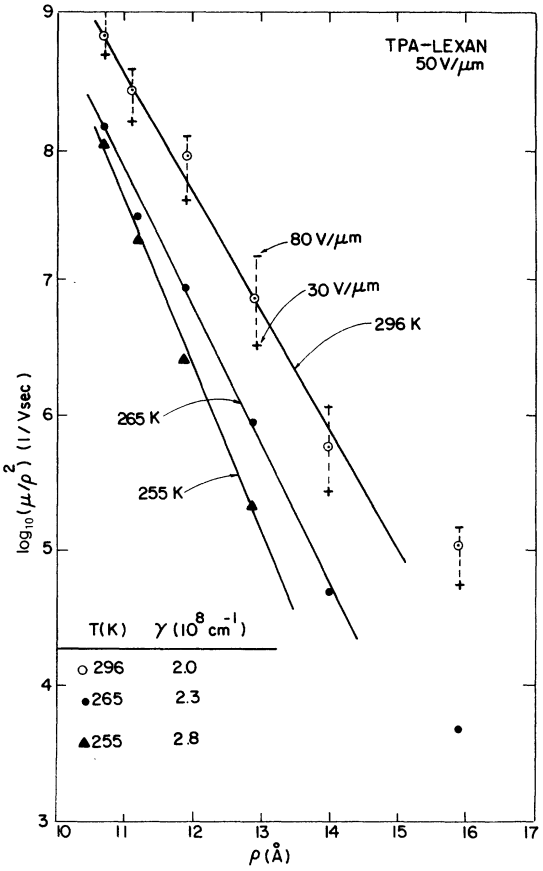

FIG. 7. Concentration dependence of the hole mobility at 50 V/μm for $T=296$, 265, and 255 K. The overlap parameters γ (slopes) are listed in the legend. For $T=296$ K the mobilities for $E=80$ V/μm (bars) and 30 V/μm (crosses) are also shown.

Figure 6 suggests the empirical relationship

$$\mu_0 \sim \rho^p \exp(-\gamma_0 \rho)^q \ . \qquad (2)$$

The strong concentration dependence of μ_0 confirms earlier interpretations that transport in molecularly doped systems occurs via a hopping process among sites associated with the dopant molecule.[4-7] The power exponents p and q cannot be determined from the data shown. To be consistent with earlier papers,[6,15] $p \cong 2$, and $q \cong 1$, is assumed for further analysis. From Fig. 6 one obtains $\gamma_0 \sim 1.5 \times 10^8$ cm^{-1}.

Figure 7 shows the variation of $\log_{10}(\mu/\rho^2)$ with hopping distance ρ for various experimental conditions. The results indicate an increase in charge localization as the temperature is lowered. No uniform field dependence of the localization parameter γ was evident at 296 K for the field range 30–80 V/μm. With an experimental accuracy of $\Delta\gamma/\gamma \sim 10\%$–$20\%$, one estimates from Fig. 7, $\partial\gamma/\partial T \sim -1 \times 10^6$ K^{-1} cm^{-1}, and the upper limit $\partial\gamma/\partial E \lesssim -50$ V^{-1}.

Figure 8 shows the field dependence of the mobility at 273 K for various TPA concentrations. With decreasing TPA concentration the field dependence becomes stronger. Defining β as slope of the straight lines in Fig. 7, one finds $\partial\beta/\partial\rho$ (273 K) $\sim 5 \times 10^4$ (V/cm)$^{-1/2}$ cm^{-1}.

The activation energy Δ exhibits a similar concentration dependence. From the Arrhenius plots shown in Fig. 9 one estimates $\partial\Delta/\partial\rho \sim 3 \times 10^6$ eV cm^{-1}. No field dependence of $\partial\Delta/\partial\rho$ was observed in the range 40–70 V/μm.

Since no field and temperature dependence is assumed in prefactor μ_0 of Eq. (1), the concentration dependence of Δ and β and the field and temperature dependence of γ are related. From Eq. (1) one finds $\partial\gamma/\partial T = -(\partial\Delta/\partial\rho)/kT^2$, and $\partial\gamma/\partial E = -(\partial\beta/\partial\rho)/2\sqrt{E}$. The experimental values

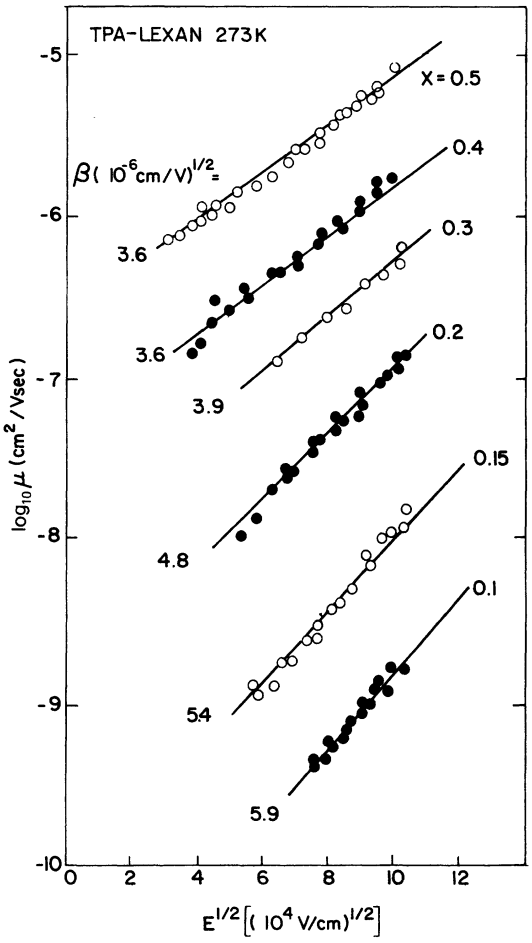

FIG. 8. Field dependence of the hole mobility at $T=273$ K for various TPA concentrations. The slopes β and the weight ratios X of TPA are listed.

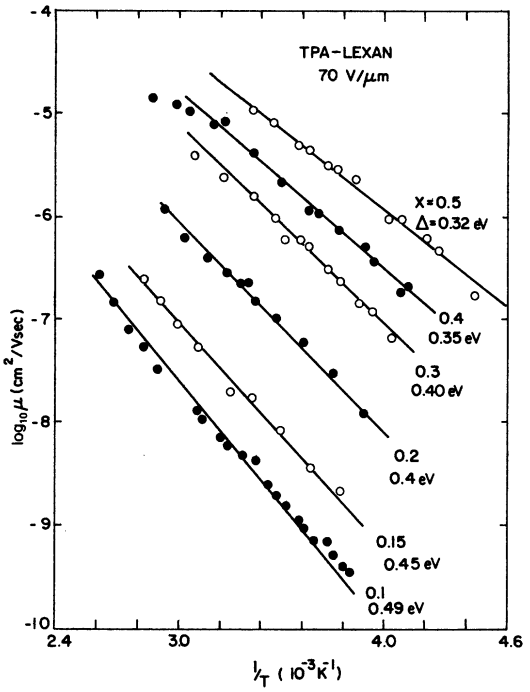

FIG. 9. Temperature dependence of the hole mobility at $E = 70$ V/μm for various TPA concentrations. The activation energies and the weight ratios X of TPA to Lexan are listed.

quoted above are indeed in reasonable agreement with these relations.

The scatter of the parameter values $E_0^{1/2}$, T_0, and a determined for samples of different concentrations was too large to unambiguously determine their concentration dependence. However, an overall increase of all three parameters with decreasing concentration was indicated. Typical variations for the concentration range 0.5–0.1 TPA are, respectively, $a \cong 4$–5 K $(\mathrm{V/cm})^{-1/2}$, $E_0^{1/2} \cong (1.7\text{–}2.0) \times 10^3$ $(\mathrm{V/cm})^{1/2}$, and $T_0 \cong 360$–400 K.

Results similar to those discussed here for TPA-doped Lexan 145 were observed for the dopant molecule N-isopropylcarbazole (NIPC). Of the three parameters introduced in Eq. (1), $E_0^{1/2}$ and a were within the range of the values obtained for TPA-Lexan, but T_0 was significantly higher (~550 K).

IV. DISCUSSION

The strong concentration dependence on the thermally activated drift mobility is evidence that hole transport in the TPA-Lexan system occurs via hopping among sites associated with the TPA molecules. Similar observations indicated hopping mechanisms for transport of holes in NIPC-Lexan[6] and electrons and holes in PVK:TNF.[5,15] On a microscopic scale, charge transport in molecularly dispersed systems can be visualized as transition of an electron from a neutral molecule to the neighboring "molecular cation" (hole transport) or from the "molecular anion" to a neighboring neutral molecule (electron transport). (The term "molecular ion" is used quite freely in this context. It includes the situation where the charge is bound rather loosely on the transport molecule and spreads substantially over neighboring matrix molecules.) This mechanism suggests that the transport properties vary strongly with the parameters of the dopant molecules. This is quite different from transport in the ordered state (molecular crystals), where for a wide range of materials electron and hole mobilities are of the order of ~1 $\mathrm{cm^2/V\,sec}$ and have similar temperature behavior. Evidently, in the crystalline state where narrow-band formation might occur, the influence of the molecular parameters on the transport properties is reduced and one cannot reasonably infer anything about charge transport in disordered solids from the corresponding crystalline data.

A. Theoretical concept

The shape of the transient current pulse (Figs. 1 and 2) indicate that the hole packet injected by the light flash undergoes a broad dispersion as it propagates through the bulk of the sample film. Under these conditions the theoretical framework introduced by Scher and Montroll[1] to analyze dispersive transient transport should be applicable. Scher and Montroll realized that trivial fluctuations in transport parameters (activation energy, hopping distance) can lead to significant fluctuations of the individual hopping times (trap-release time for extended-state conduction) due to the typically large argument of the exponential functions that describe the charge transfer. For instance, a fluctuation of 1 Å for an average hopping distance of 10 Å changes the hopping time by about one order of magnitude (compare Fig. 7). In the present system the hopping sites are molecular entities of dimensions comparable to the hopping distance, and therefore fluctuations of the molecular orientation constitute an additional source of dispersion. If the fluctuations of the individual hopping times extend into the time range of the experiment, i.e., the transit time t_T, the statistics describing the kinetics of the dispersion become non-Gaussian. This leads to novel features of carrier transport. For the "ideal" case of non-Gaussian transport, where the dispersion of the carrier packet is solely due to fluctuations of bulk parameters, Scher and Montroll find

$$I(t) \propto \begin{cases} t^{-(1-\alpha)}, & t < t_T, \\ t^{-(1+\alpha)}, & t > t_T, \end{cases} \tag{3}$$

where

$$t_T = cW_0^{-1}[L/l(E)]^{1/\alpha} \exp(\Delta_0/kT). \tag{4}$$

α is a measure of the dispersion and assumes a value between 0 and 1, c is a constant of the order of unity, and $l(E)$ is the mean (field dependent) carrier displacement per hop in direction of the applied field E and L is the sample thickness. The "transit time" t_T can be determined from the intercept of the tangents approximating the transient current in units $\log_{10} I$ vs $\log_{10} t$ (Figs. 1 and 2). For temperature-independent fluctuations in the hopping distance[1]

$$\alpha \cong (\rho_0/\rho)\{\ln[L/l(E)]\}^{2/3}, \tag{5}$$

where $2\rho_0$ is the Bohr radius of the charge localization. For an exponential distribution of trap-release energies[12] $N(\epsilon) \propto \exp(-\epsilon/kT_0)$,

$$\alpha = T/T_0. \tag{6}$$

B. Dispersion parameter α

Equation (3) describes the current shape for the "ideal" case of non-Gaussian transport independent of the actual source of dispersion. In the TPA-Lexan system, surface trapping and/or space-charge in the depletion layer near the surface influence the shape of the current pulse which obscure the determination of the dispersion parameter α from the current trace. In fact, examination of the traces in Figs. 1 and 2 shows that the α values determined from the pre and post transit time current shape are different rather than being equal. Typically, $\alpha(t < t_T) > \alpha(t > t_T)$.

A recent expansion of the theory includes the contribution of charge release from an ideal surfact at $X = 0$ to the transient current.[9] The treatment shows that surface effects can significantly modify the initial shape of the current pulse. Depending upon the release time and density of surface traps in relation to transit time and concentration of the charge in transit, surface effects can produce cusps or plateaus in $I(t)$ for $t < t_T$ and increase the dispersion for $t > t_T$. The latter effect, however, is much less significant, which is in qualitative agreement with the data shown in Figs. 1 and 2. Typically, the α value obtained from $I(t > t_T)$ is a lower limit to the bulk dispersion parameter. From Figs. 1 and 2 we estimate $\alpha > 0.35$.

In the non-Gaussian regime the transit time depends on sample thickness in a manner related to the dispersion [Eq. (4)]. For a-As_2Se_3 and a-Se, this correlation was examined for a wide range of sample thicknesses.[9,10] A similar study was carried out for the discussed doped polymers. The interpretation of the results, however, is problematic, since by solvent casting, it is difficult to vary the sample thickness by an appreciable amount and maintain a uniform molecular solution. Sequential coatings of thin layers to build up a thick layer could introduce interfacial traps which cause an apparent decrease of the mobility as the layer thickness increases. These effects are difficult to separate from a thickness dependence of the mobility which is due to the statistics of the transport process, Eq. (4). Figure 10 shows the field dependence of the mobility for 0.3 TPA for various sample thicknesses. The 33-μm sample was prepared by two coatings of ~15 μm each. Within the mentioned limitations of these measurements one estimates $\alpha \sim 0.6$.

An additional estimate of α can be obtained from the concentration dependence of t_T. By combining Eqs. (4) and (5) and using the experimental result $t_T \propto \exp(\gamma\rho)$ (Fig. 7) one derives

$$\gamma = (1/\rho_0)\{\ln[L/l(E)]\}^{1/3} \tag{7}$$

and

$$\alpha = (1/\gamma\rho)\ln[L/l(E)]. \tag{8}$$

Hence α can be calculated using the experimentally determined localization parameter γ. From Fig. 7, $\gamma \sim 2 \times 10^8$ cm^{-1} at 296 K. For $l \sim 0.1\rho$, $L = 10$ μm, one finds $\alpha = 0.58$.

Equation (8) predicts that the dispersion increases with decreasing concentration, and that it is temperature and field dependent in a manner dictated by γ and l. While these qualitative trends are indicated in the experimental results, the predicted variations are somewhat too large. This

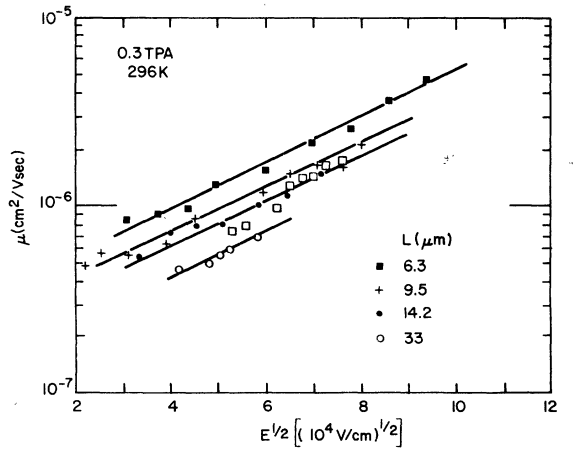

FIG. 10. Field dependence of mobility for 0.3 TPA for various sample thicknesses. $T = 296$ K.

is expected since several sources are likely to contribute to the dispersion with the resulting effect that α becomes insensitive to variations of experimental parameters. However, the reasonable agreement of the α values determined from the different experiments (current shape, thickness, and concentration dependence) suggest that Eqs. (3)–(5) are quite satisfactory approximations for a qualitative analysis of hole transients in TPA-Lexan.

C. Field and temperature dependence

In a conventional semiconductor where charge transport occurs in extended states the observed $\exp(aE^{1/2}/kT)$ field and temperature dependence of the mobility would indicate a Poole-Frenkel mechanism[19] in which the carrier escapes from a charged trapping center into the conduction band under the influence of the applied field. In this model, $a_{PF}E^{1/2}$ is the field-induced lowering of the Coulomb barrier where $a_{PF}=(e/\pi\epsilon\epsilon_0)^{1/2}\sim 5$ $(\mathrm{cm/V})^{1/2}\mathrm{K}$ is the Poole-Frenkel coefficient for $\epsilon=3$. This value is in remarkable agreement with the average value $a\sim 4.6$ $(\mathrm{cm}/V)^{1/2}\mathrm{K}$ from our experiments. A similar excellent formal agreement with the Poole-Frenkel mechanism has been observed by Gill for electron and hole transport for the PVK:TNF charge transfer complex.[15] However, the basic assumptions leading to the Poole-Frenkel model are questionable when applied to the doped polymer systems discussed and despite the striking experimental agreement, this model is not likely to provide the correct interpretation of the field dependence of the drift mobility. Similar conclusions were advanced by Gill for the case of PVK:TNF.

In the Scher-Montroll theory, barrier lowering effects can be incorporated in the mean displacement per hop $l(E)$. For hole transport in a-As_2Se_3 the experiments indicate that for $E<10$–15 V/μm, and $T\gtrsim 270$ K the mean displacement increases in proportion to the applied field, $l(E)\propto E$, i.e., $t_T\propto(L/E)^{1/\alpha}$. At higher fields the field dependence becomes steeper, and it has been shown that an expression of the form

$$\mu=\frac{L}{t_T E}\sim W_0\frac{L^{1-1/\alpha}}{E}\left(\sinh\frac{e\rho E}{2kT}\right)^{1/\alpha}\exp\left(\frac{-\Delta_0}{kT}\right) \quad (9)$$

can account for the data on a-As_2Se_3 for a wide field and temperature range with reasonable values for the parameters α and ρ.[20] It is tempting then to apply Eq. (9) to the present system where the hopping distance can independently be estimated from the TPA concentration. The derivation of Eq. (9) assumes that the hopping probability in field direction increases exponentially as $\exp(e\rho E/2kT)$ and that its saturation occurs at fields much higher than experimentally applicable.[20] [In Eq. (9) the conventional definition of the mobility is used for easier comparison with expressions given in the literature. One has to keep in mind that because of the L dependence the mobility loses its conventional meaning in non-Gaussian transport.]

The difference between earlier barrier lowering formulas[21,22] and Eq. (9) is the presence of the power exponent $1/\alpha$ which is a consequence of Scher and Montroll's treatment of dispersive transport in three dimensions while the previous models, although incorporating barrier fluctuations,[22] were restricted to a one-dimensional analysis. A treatment similar to that leading to Eq. (9) has been suggested by Maitra.[23] At high fields the one- and three-dimensional treatment become formally identical since the field introduces a large spacial asymmetry. At low fields, however, the power exponent $1/\alpha$ plays a significant role. While for the one-dimensional treatments the mobility approaches a field-independent value, Eq. (9) predicts

$$\mu\propto(1/E)(e\rho E/2kT)^{1/\alpha}\exp(-\Delta_0/kT)\,. \quad (10)$$

The significance of a calculation in three dimensions for the low-field data has been amply demonstrated.[9] At high fields Eq. (9) reduces to

$$\mu\propto(1/E)\exp(e\rho E/2k\alpha T)\exp(-\Delta_0/kT)\,. \quad (11)$$

Note that $1/\alpha>1$ corresponds to the dispersion parameter $s>1$ in the one-dimensional treatment.[22]

The Arrhenius plots for various applied fields intersect at a finite temperature T_0 rather than $T=0$ (see Fig. 4, for example). Hence for $T<T_0$ the temperature dependence of the mobility can be described by an effective temperature $1/T-1/T_0$, which is apparent from the phenomenological expression Eq. (1).

It is suggested that appearance of an effective temperature results from a temperature dependence of the dispersion parameter α. A possible source for this dependence is a distribution of energy levels as is exemplified by Eq. (6) for the case of an exponential distribution. Comparison of the high-field approximation Eq. (10) with the phenomenological expression Eq. (1) suggests α to be of the general form

$$\alpha\cong\alpha_0/(1-T/T_0)\,. \quad (12)$$

The applicability of this relation is subject to the conditions $0<\alpha<1$ and $T<T_0$. Introducing Eq. (12) in Eq. (13) leads to

$$\mu\propto\frac{1}{E}\exp\left[\frac{e\rho}{2k\alpha_0}(E-E_0)\left(\frac{1}{T}-\frac{1}{T_0}\right)\right]\exp\left(\frac{-\Delta_0}{kT_0}\right), \quad (13)$$

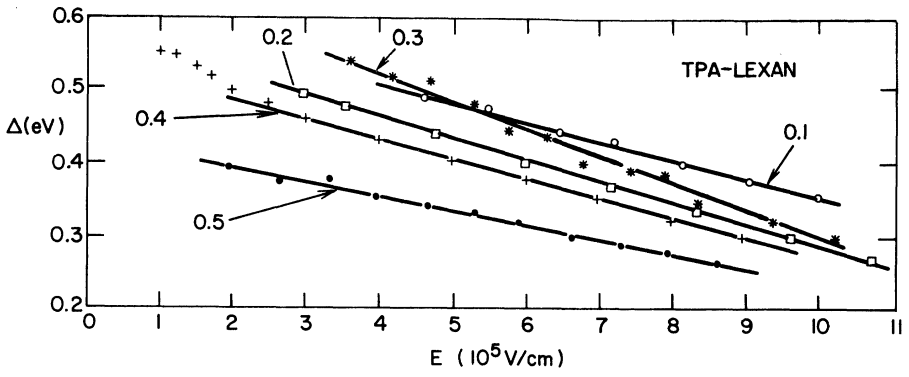

FIG. 11. Linear field dependence of activation energy for samples of different TPA concentration.

where $E_0 = 2\alpha_0\Delta_0/e\rho$. In the high-field limit the activation energy is given by

$$\Delta(E) = \Delta_0 - (e\rho/2\alpha_0)E . \quad (14)$$

Over the limited field range typical of these experiments, Eqs. (1) and (9) are expected to give similar results. With the dispersion α being temperature dependent, Eq. (9) contains five parameters ρ, α_0, T_0, Δ_0, and W_0. Of these only the first three are significant since W_0 is only a scaling parameter and Δ_0 has no influence upon the (temperature dependent) curvature of the μ-vs-E plots. This curvature, however, is strongly sensitive to the choice of α_0, T_0, and ρ. Now, ρ can be calculated from the concentration of the TPA molecules. With ρ fixed, α_0 can be determined from the field dependence of the activation energy, Eq. (14). This leaves T_0 as the only parameter available to adjust the curvature of the μ-vs-E plots over the entire temperature range where Eq. (12) holds. With T_0 and α_0 so determined, the calculated dispersion parameter $\alpha(T)$, Eq. (12) should then match the values estimated from the current shape and the thickness and concentration dependence of the transit time. This procedure is now applied to several TPA samples. First, the linear field dependence of the activation energy is shown in Fig. 11. From this figure, the slope $\rho/2\alpha_0$ can be obtained for each sample. Using 0.5 TPA as an example one has $\rho = 10.7$ Å from the molecule concentration, $\rho/2\alpha_0 = 20$ Å from Fig. 11, and therefore $\alpha_0 = 0.26$. With these values Eq. (9) has been fitted to the data for $T_0 = 455$ K. Figure 12 compares the experimental results with the calculated mobilities in a plot of $\log_{10}\mu$ vs $\log_{10}E$. The agreement is remarkable over a wide temperature and field range. The dispersion parameter calculated with the fitted α_0 and T_0 decreases from ~0.74 of 297 K to 0.44 at 185 K. Although the room-temperature value is somewhat large the overall temperature variation is certainly consistent with the experimental results. Figure 13 compares the fitted curves with the results for a 0.3-TPA sample. Good fits were also obtained for samples of still lower concentration but the experimental field range for these samples is so limited that the fits do not provide a meaningful

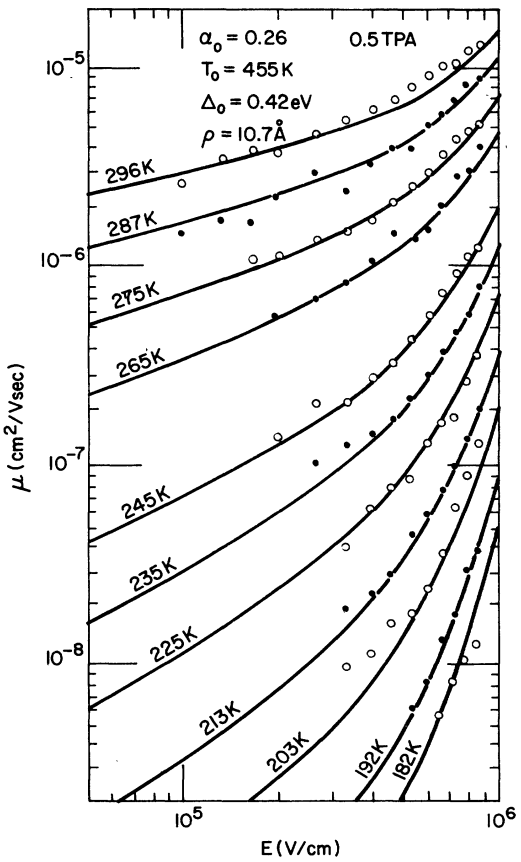

FIG. 12. μ vs E for 0.5 TPA at various temperatures. Curves were calculated from Eq. (9) using parameters listed in the figures.

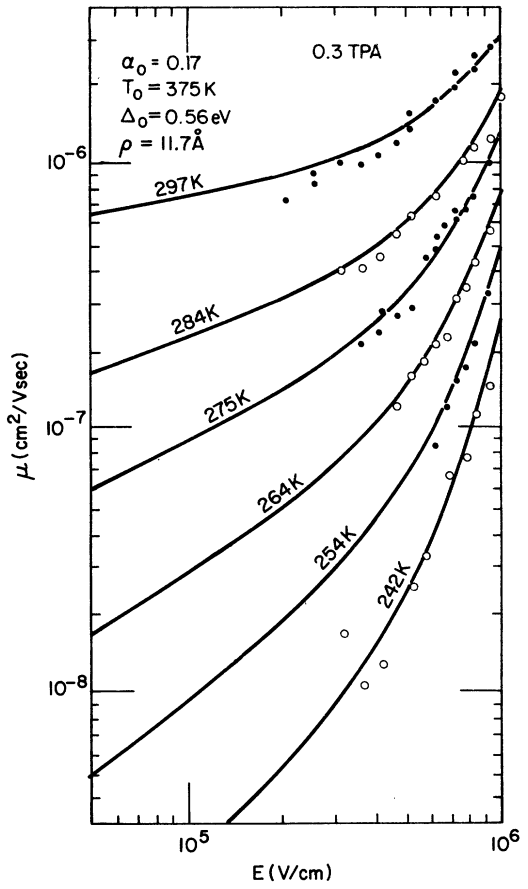

FIG. 13. μ vs E for 0.3 TPA. See caption, Fig. 12.

test for the applicability of Eq. (9). The dashed lines in Fig. 3 show the fitted curves for the 0.4-TPA sample. It is seen that in the $\log_{10}\mu$-vs-$E^{1/2}$ plot Eqs. (1) and (9) indeed yield very similar results in the field range spanned by the experimental results. A more stringent test of Eq. (9) requires data at much lower fields than experimentally feasible in these experiments. The low end of the field range is determined by the signal-to-noise ratio which decreases because of decreasing carrier velocity and carrier generation efficiency. The latter is temperature and field dependent and decreases exponentially with increasing hopping distance ρ.[6] The algebraic field dependence predicted by Eq. (9) for low fields could be observed for hole transport in a-As_2Se_3 in the field range 1-10 V/μm. In this case[9,20] $\rho \sim 40$ Å and $\alpha \sim 0.5$ (temperature independent).

D. $\gamma(E,T)$ and $\Delta(\rho),\beta(\rho)$

The observed variation of the activation energy Δ and field dependence β with intersite distance ρ, and the field and temperature dependence of the charge localization γ are related. It is, therefore, not possible to separate the two effects and pinpoint the actual source for these dependences without further experimental information. Although several mechanisms for either effect can readily be proposed (trapping, disorder, molecular vibrations), such a discussion appears rather speculative at present and will be deferred until more detailed studies are available that relate sample morphology, impurities, and parameters of host polymer and transport molecule to the parameters introduced in Eq. (1) or Eq. (9). A detailed comparison of the transport data for PVK:TNF, NIPC-Lexan, and TPA-Lexan might be a first step in this direction.

V. CONCLUSIONS

Hole transport in triphenylamine-doped polycarbonate polymer, TPA-Lexan, proceeds by hopping among localized sites associated with the TPA molecule. Representative values for the drift mobility at room temperature, 50 V/μm applied field, and a 10-μm thick sample are $\mu \sim 7 \times 10^{-6}$ cm^2/V sec for 0.5 TPA and $\mu \sim 1.5 \times 10^{-9}$ cm^2/V sec for 0.1 TPA.

Equation (1) provides a useful phenomenological description of the drift mobility over the experimentally accessed field range of 20–100 V/μm and temperature range of 100 K around room temperature. The parameters introduced in Eq. (1) slightly increase with decreasing concentration. For the range 0.5–0.1 TPA, their respective variations are $a \sim 4$–5 K (V/cm)$^{-1/2}$, $E_0^{1/2} \sim (1.7$–$2.0) \times 10^3$ (V/cm)$^{1/2}$, and $T_0 \sim 360$–400 K. These temperatures T_0 are significantly lower than those obtained from a similar analysis of electron and hole transport in the charge transfer complex of PVK:TNF.[15]

The activation energy Δ and the field dependence at constant temperature (slope β) increase with decreasing TPA concentration and, related to this dependence the charge localization γ appears to increase as the temperature is lowered. The respective variations are of the order of magnitudes $\partial\gamma/\partial T \sim -1 \times 10^6$ K^{-1} cm^{-1}, $\partial\gamma/\partial E < -50$ V^{-1}, $\partial\beta/\partial\rho$ (271 K) $\sim 5 \times 10^4$ (V/cm)$^{-1/2}$ cm^{-1}, and $\partial\Delta/\partial\rho \sim 3 \times 10^6$ eV cm^{-1}. These variations are consistent with the concentration dependence of the parameters a, T_0, and $E_0^{1/2}$.

The Scher-Montroll theory of stochastic non-Gaussian transport provides a consistent interpretation of all experimental results if barrier lowering and temperature-dependent dispersion are formally introduced in the theoretical expression for the transit time t_T, Eq. (3). A tempera-

ture-dependent dispersion could arise, for instance, from a fluctuation of hopping energies in which case the characteristic temperature T_0, Eq. (1), provides a measure for that spread.

The detailed study of electronic transport in molecularly doped organic polymers furnishes an important additional test for transport mechanisms proposed in other disordered solids. That Eq. (9) provides a consistent interpretation of the experimental results for doped polymers and the chalcogenide glass a-As_2Se_3 suggests that the transport mechanism in these materials may be very similar.

ACKNOWLEDGMENTS

Many thanks are due to S. Grammatica for his careful preparation of the samples, D. Leopold for the measurement of the film concentrations, and A. Wilson for the assistance in writing the computer program. Numerous discussions with Dr. H. Scher which clarified many of the aspects of the Scher-Montroll theory are greatly appreciated. Finally, thanks are due to Dr. J. Mort who introduced me to the interesting field of molecularly doped polymers and whose continuing interest was pertinent for the completion of these studies.

[1]H. Scher and F. W. Montroll, Phys. Rev. B 12, 2455 (1975).
[2]H. Scher, in *Photoconductivity and Related Phenomena*, edited by J. Mort and D. M. Pai (American Elsevier, New York, 1976), p. 71.
[3]H. Hoegl, J. Phys. Chem. 69, 755 (1965).
[4]W. Mehl and N. E. Wolff, J. Phys. Chem. Solids 25, 1221 (1964).
[5]W. D. Gill, in *Amorphous and Liquid Semiconductors*, edited by J. Stuke and W. Brenig (Taylor and Francis, London, 1974), p. 901.
[6]J. Mort, G. Pfister, and S. Grammatica, Solid State Commun. 18, 693 (1976).
[7]G. Pfister, S. Grammatica, and J. Mort, Phys. Rev. Lett. 37, 1360 (1976).
[8]G. Pfister, Phys. Rev. Lett. 33, 1474 (1974).
[9]G. Pfister and H. Scher, Phys. Rev. B 15, 2062 (1977).
[10]G. Pfister, Phys. Rev. Lett. 36, 271 (1976).
[11]M. Silver and L. Cohen, Phys. Rev. B 15, 3276 (1977).
[12]H. Scher (private communication).
[13]F. Schmidlin, Bull. Am. Phys. Soc. 22, 346 (1977).
[14]J. Noolandi, Bull. Am. Phys. Soc. 22, 434 (1977).
[15]W. D. Gill, J. Appl. Phys. 43, 5033 (1972).
[16]R. Enck and G. Pfister, in *Photoconductivity and Related Phenomena*, edited by J. Mort and D. M. Pai (American Elsevier, New York, 1976), p. 215.
[17]M. Silver, K. S. Dy, and I. L. Huang, Phys. Rev. Lett. 27, 21 (1971).
[18]W. M. Prest (private communication).
[19]J. Frenkel, Phys. Rev. 54, 647 (1938).
[20]G. Pfister (unpublished).
[21]B. G. Bagley, Solid State Commun. 8, 345 (1970).
[22]K. Funabashi and B. N. Rao, J. Chem. Phys. 64, 1561 (1976).
[23]S. Maitra (private communication).